POLISH POLAR RESEARCH
vol. 44 no. 3, pp. 227–248, 2023 DOI: 10.24425/ppr.2023.144542

Contemporary landscape transformation in a small Arctic catchment, Bratteggdalen, Svalbard

Aleksandra WOŁOSZYN* and Marek KASPRZAK

Institute of Geography and Regional Development, University of Wrocław,
pl. Uniwersytecki 1, 50-137 Wrocław, Poland

* *corresponding author <aleksandra.woloszyn@uwr.edu.pl>*

Abstract: Small Arctic catchments that are sensitive to climate change reinforced by Arctic amplification remain poorly studied. Since the end of the Little Ice Age (LIA) glaciers on Svalbard have been retreating, and thus, many catchments have transformed from glaciated or partly glaciated to ice-free conditions. Our study focuses on changes that have occurred since the end of the LIA in a small High Arctic mountain catchment, Bratteggdalen. In this study, we traced changes in the Bratteggbreen glacier areal extent since 1976 with parallel vegetation analysis using Landsat and Sentinel data. The geomorphology of Bratteggdalen was mapped and basic morphometric analyses, such as long profile, hypsometric curve, slope and aspect orientation analyses were carried out. We also present a map of landforms in Bratteggdalen based on a fieldwork in 2018 and an analysis of orthophotomaps. Through this research, we enhance the knowledge of small catchments in polar regions.

Keywords: Arctic, Spitsbergen, small catchment, geomorphology, environmental changes.

Introduction

Small mountain catchments in the High Arctic are indicators of rapid environmental changes due to Arctic amplification (Serreze and Barry 2011; Francis and Vavrus 2012; Goosse *et al.* 2018; Szafraniec 2018; Hanssen-Bauer *et al.* 2019; Fang *et al.* 2022). Moreover, among the High Arctic, Svalbard mean annual air temperatures are noticeably higher (Eckerstorfer and Christiansen 2011). While it is difficult to specify the watershed of small drainage basins, it can be assumed that these areas are not conducive to snow accretion. Glaciers in small, High Arctic catchments are drastically thinning and retreating (Noël *et al.* 2020; Geyman *et al.* 2022a; Małecki 2022). The rapid glaciological and hydrological changes as well as active layer deepening lead to enhanced surface and slope processes in the summer months (Hanssen-Bauer *et al.* 2019). These, in turn, are strongly influenced by ground thermics, and thus, by increasing active layer depth thaw in the summer months (Christiansen *et al.* 2010, 2019; Peng *et al.* 2018; Strand *et al.* 2021). Modern-day factors, which increase snow ablation and permafrost thawing, cause changes in surface and groundwater runoff regimes (Dugan *et al.* 2009; Lamoureux *et al.* 2014; Owczarek *et al.* 2014; Lafrenière and Lamoureux 2019).

Bratteggdalen (nor. *dalen* means valley) is a small mountain catchment in Wedel Jarlsberg Land, on the southwestern coast of Spitsbergen. The Stanisław Baranowski Polar Station is located at the mouth of this valley, and it is also in the vicinity of the intensively studied glaciated valley of Werenskioldbreen (Ignatiuk *et al.* 2022). Consequently, Bratteggdalen is one of the most investigated sites in this part of Spitsbergen. Research and observations carried out there have formed the core for publications on hydrogeology (Marszałek and Wąsik 2013; Marszałek *et al.* 2013), mass movements and slope processes (Jahn 1967; Jokiel *et al.* 2012; Kasprzak 2015; Senderak and Wąsowski 2016; Senderak *et al.* 2019) and lake water chemistry (Marszałek and Wąsik 2013; Górniak *et al.* 2015; Marszałek and Górniak 2017). However, the surface morphology and surface conditions have not been explored in detail (Brázdil *et al.* 1988; Migoń and Kasprzak 2013).

This paper aims to give the broadest possible topographic characteristics of the catchment of Bratteggelva (nor. *elva* means river). In this work, we present a detailed geomorphological and surficial geologic map as well as high-resolution digital terrain models (DTMs). The DTMs are derived from airborne laser scanning or photogrammetric processing of aerial photographs (Dudek and Pętlicki 2021; Geyman *et al.* 2022a). Furthermore, on a basis of available LANDSAT (USGS 1976–2017) and Sentinel (2018–2021) satellite imagery, we assess the scale of landscape change. The information provided in this paper may be useful not only for further research work in Bratteggdalen but also as a reference for studies of other small mountain catchments in the High Arctic.

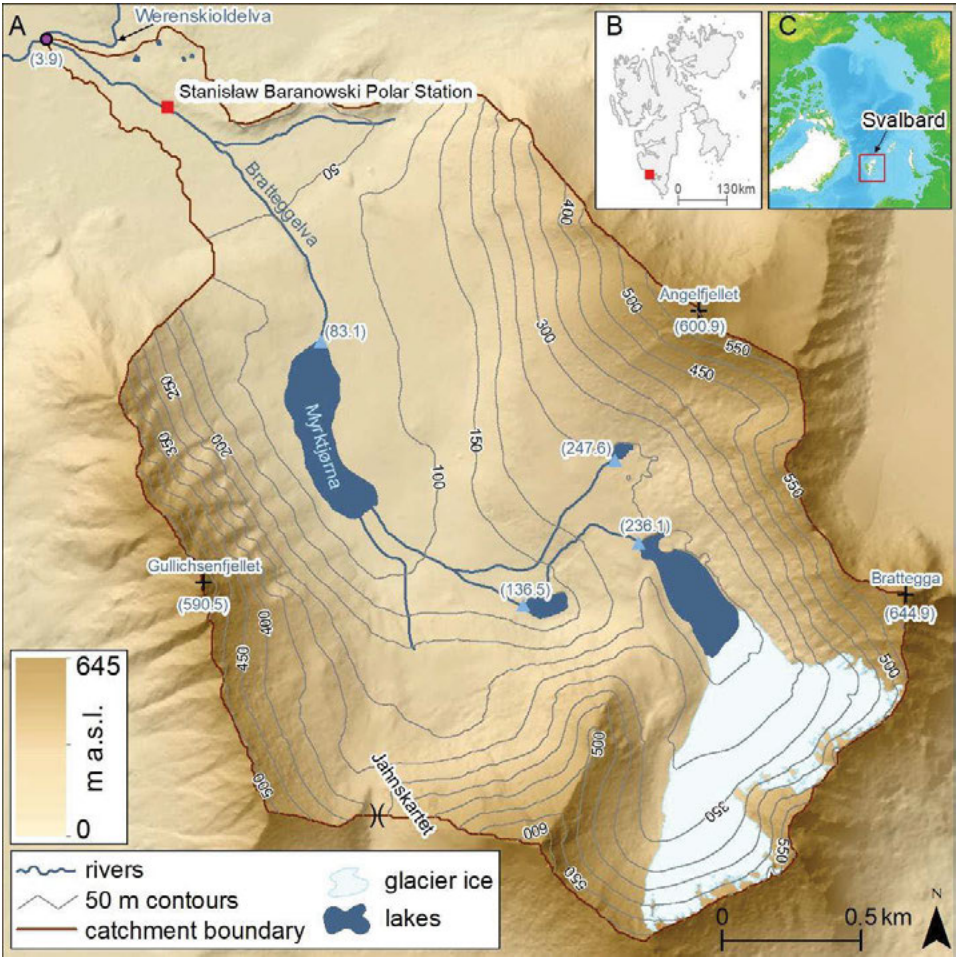

Fig. 1. Overview map of the study area: **A** - the Bratteggelva catchment, modified from ArcticDEM (Porter *et al.* 2018), contours based on digital elevation model; **B** - map of Svalbard, location of study area indicated by red square (Modified from Norwegian Polar Institute 2014a); **C** - polar projection map of the Arctic Ocean (data provided by Arctic-SDI geoportal).

Study area

Bratteggdalen is a small (7.44 km^2) catchment located in Wedel Jarlsberg Land, SW Spitsbergen (Fig. 1). The elevation of the catchment area range from 4 to 645 m a.s.l. with a north-northwest flow direction. The bedrock of the catchment is mainly composed of the Eimfjellet Group (Fig. 2), including amphibolites and mica schists of the Bratteggdalen Formation, and white and green quartzites of the Guliksenfjellet Formation (Czerny *et al.* 1993; Manecki *et al.* 1993; Majka *et al.* 2010). The surface morphology of the lower part of the valley is dominated by raised marine beaches with bedrock cropping out occasionally up to 100 m a.s.l. (Karczewski 1984). The catchment has continuous permafrost, verified by geophysical surveys (Kasprzak 2015, 2020). In this part, the river is braided (Kowalska and Sroka 2008; Owczarek *et al.* 2014). The central part of the valley is dominated by a series of talus cones on the western side of the catchment and a long, slightly sloping solifluction area on the opposite side.

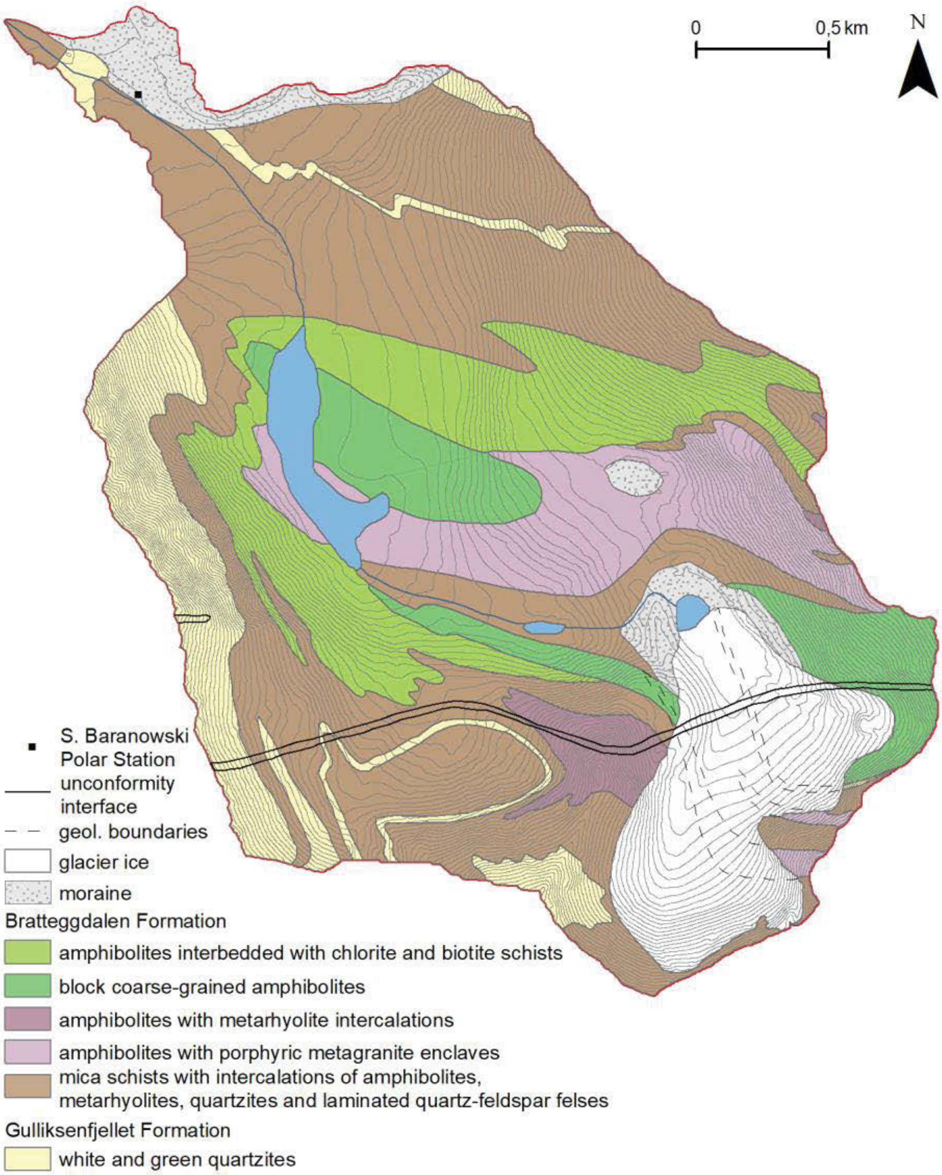

Fig. 2. Geological map of the study area modified from Czerny *et al.* (1993). Note different extent of the glacier and lakes as compared to Fig. 1, which is due to considerably earlier time of mapping.

The local climate is cold but relatively mild due to the influence of the West Spitsbergen Current (Piechura and Walczowski 2009; Walczowski and Piechura 2011). A 40-year-long meteorological data series from 1979 to 2018 is available from the Polish Polar Station in Hornsund 14 km from the study site. Based on the meteorological record, the mean annual air temperatures of the Hornsund area is estimated at −3.7°C (extreme values −35.9°C on 16th January 1981 and 15.6°C on 31st of July 2015) with March as the coldest month (mean temp. −10.2°C) and July as the warmest (mean temp. 4.6°C) (Wawrzyniak and Osuch 2020). A meteorological station was installed in Bratteggdalen from 2005 to 2011 and showed a difference of +0.6°C in mean annual air temperatures, compared to the Hornsund data for the same time period (Pereyma *et al.* 2013). Pereyma *et al.* (2013) give values ranging from 20 mm to 120 mm as a monthly precipitation sum and highlight that precipitation is highly variable within the research area.

Bratteggelva forms a lotic-lentic system with three lakes (Górniak *et al.* 2012). Bratteggelva flows into the Werenskioldelva at 4 m a.s.l. (Fig. 1). The middle part of the Bratteggdalen contains two lakes that are located on the Bratteggelva flow (Fig. 1). The first one is unnamed (outlet at 136.5 m a.s.l.). According to Marszałek and Górniak (2017), it is up to 6.7 m deep and covers 0.013 km^2. The second one is Myrktjørna (outlet at 83 m a.s.l.). It is up to 6.9 m deep and covers 0.136 km^2.

In the upper part of the catchment, a retreating cirque glacier Bratteggbreen (nor. *breen* means glacier) is located. It has well-preserved LIA frontal moraines (Migoń and Kasprzak 2013). Jania (1988) classified Bratteggbreen as a polythermal land-terminating valley glacier where glacial erosion occurs only under the central part of the glacier. The glacier front ends in an unnamed lake (0.091 km^2, 236 m a.s.l.), which is up to 40.3 m deep (Marszałek and Górniak 2017), from which Bratteggelva flows (Fig. 1). On the Angellfjellet slope, a small unnamed lake (0.004 km^2, 247 m a.s.l.) surrounded by organogenic accumulation is located.

Methods

Research in this study was based mainly on the remote sensing analysis supported with fieldwork in the summer of 2018. The geomorphological map was generated in ESRI ArcMap 10.6.1 and is based on orthophotomap derived from aerial photos from 2011 provided by the Norwegian Polar Institute as well as field mapping and photo documentation carried out during the fieldwork. The map follows the standard unified key to the detailed geomorphological map of the world (Gilewska 1968).

Geomorphometric analyses, such as slope, aspect, hypsometric curve and long profile, were carried out based on the modified ArcticDEM digital elevation model of 2 m resolution (Porter *et al.* 2018). Modifications of the digital elevation model (DEM) were undertaken in the upper part of the valley above the glacier with the northern to northwestern aspect, by deleting false area and replenishing it with statistical methods, *i.e.*, the nearest neighbor, followed by focal statistics. We carried out a substraction of two DEMs (DEMs of Difference, DoD) with a 20 m resolution from 1936 (Geyman *et al.* 2022b) and a 20 m resolution from 1990s (Norwegian Polar Institute 2014b) to measure elevation change. Changes in the Bratteggbreen were investigated based on LANDSAT data provided by the United States Geological Survey (Landsat 1976, 1979, 1980, 1983, 1985, 1988, 1990, 1993, 2010, 2014, 2016, 2017; www.earthexplorer.usgs.gov/ accessed 25.05.2022) and by the European Space Agency SentinelHub EOBrowser (Sentinel 2018, 2020, 2021; https://apps.sentinel-hub.com/eo-browser/ accessed 26.05.2022). The glacier surface on each satellite image was mapped in ArcMap.

To trace vegetation cover, spectral and quality changes in temporal variability, we used the Normalized Difference Vegetation Index (NDVI). The NDVI for the years 1976, 1980, 1990, 2010 and 2020 was calculated using the raster calculator tool with standard formula (Bhatt *et al.* 2021):

$$NDVI = \frac{NIR - RED}{NIR + RED}$$

We used the following bands for calculating the vegetation index: the years 1976 and 1980 bands 6 and 7 (Markham and Barker 1983), for 1990 and 2010 bands 3 and 4 (Johansen and Tømmervik 2014) and for 2020 bands 8 and 4 (Phiri *et al*. 2020). The satellite data differ in spatial resolution from 60 m to 5 m accuracy. The presence of a shadow and/or clouds on the Gullichsenfjellet slope (Fig. 1) prevents the analysis of this part of the catchment. Thus this data was excluded from the analyses. All GIS analyses were carried out in ArcMap 10.6.1.

Results

Valley morphology. — The Bratteggdalen is 4.5 km long and its mean width, *i.e.*, the ratio of the catchment area to its maximum length, is 1.64 km. The course of Bratteggelva (Fig. 1) in the upper part of the valley is NW orientated, then shifts to WSW and then continues in NW direction until it flows to Werenskioldelva. In the long valley profile (Fig. 3A), a stepped structure with three distinguishing levels can be observed. The topmost one forms the upper part of the valley with the glacier and its landforms ending with the Bratteggelva outflow. Well-preserved lateral and frontal moraines surround the glacier (Fig. 4). In the 1970s, there was a small pond on the western moraine (Szponar 1989) indicating the presence of an ice core within. The second step is located at *ca.* 80 m a.s.l. where the river is cutting into the bedrock. From the river outflow from Myrktjørna, deep erosional gorge is visible over the next *ca.* 600 m down the valley (Figs. 4 and 5).

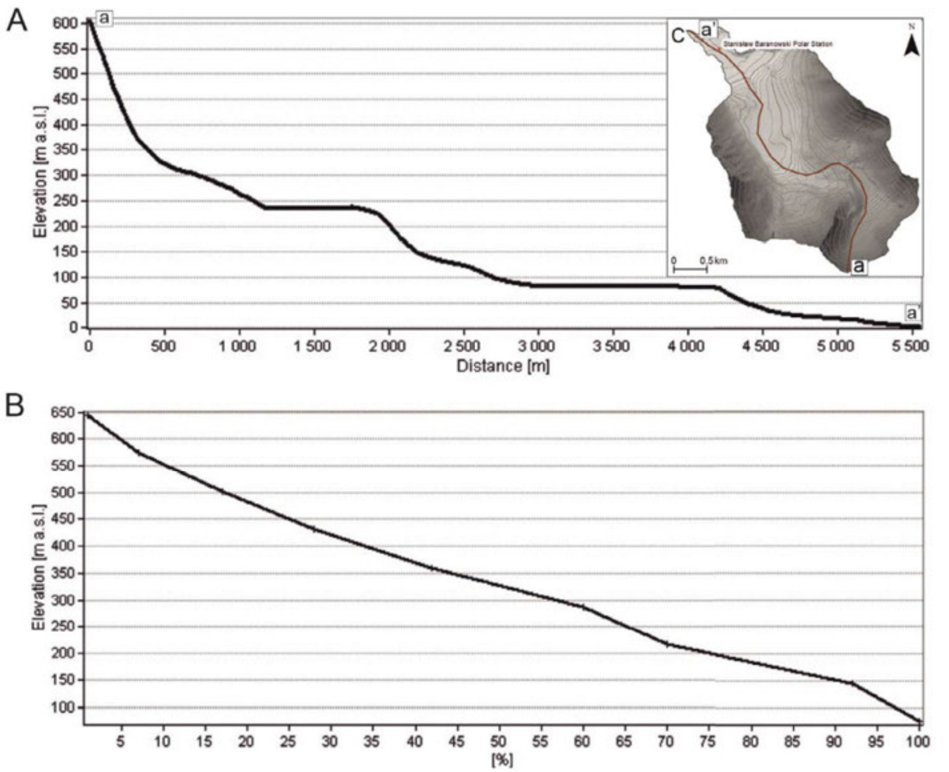

Fig. 3. Longitudinal profile (**A**), map showing location of the profile (**C**) and hypsometric curve (**B**) of the Bratteggelva catchment, based on digital elevation model.

A cumulated hypsometric curve is presented in Fig. 3B. In regard of the aspect (Fig. 6A), the catchment is split into two parts by the boundary following the NW-SE direction, from which half of it is orientated to the East and the other to the West. Slope values (Fig. 6B) vary from low values <4° up to 12° in the valley bottom to numbers >36° above 100 m a.s.l, with a mean catchment slope of 22°. Noteworthy, there are three flattened areas, visible as green patches in Fig. 6B, one on the Angellfjellet slope and one at the Jahnskaret continuation, which could be possible locations for snow accumulation and glacier formation during colder periods. The third flat surface, at the prolongation of the glacier axis, is likely shaped by a former glacial advance, evidenced by the presence of an old terminal moraine, labelled as 'older moraine' in Fig. 4.

Landforms. — The map of landforms and surface materials shown on Fig. 4 presents the Bratteggelva catchment in a geomorphological approach. Well-shaped solifluction lobes and stripes are present in large parts of the catchment. In the central part of the valley, seven talus cones (Fig. 7B) terminate on the lake shore of Myrktjørna. The DoD (Fig. 8) illustrates material loss in the higher part of the Gullichsenfjellet slope and gain in the lower part. The depicted material

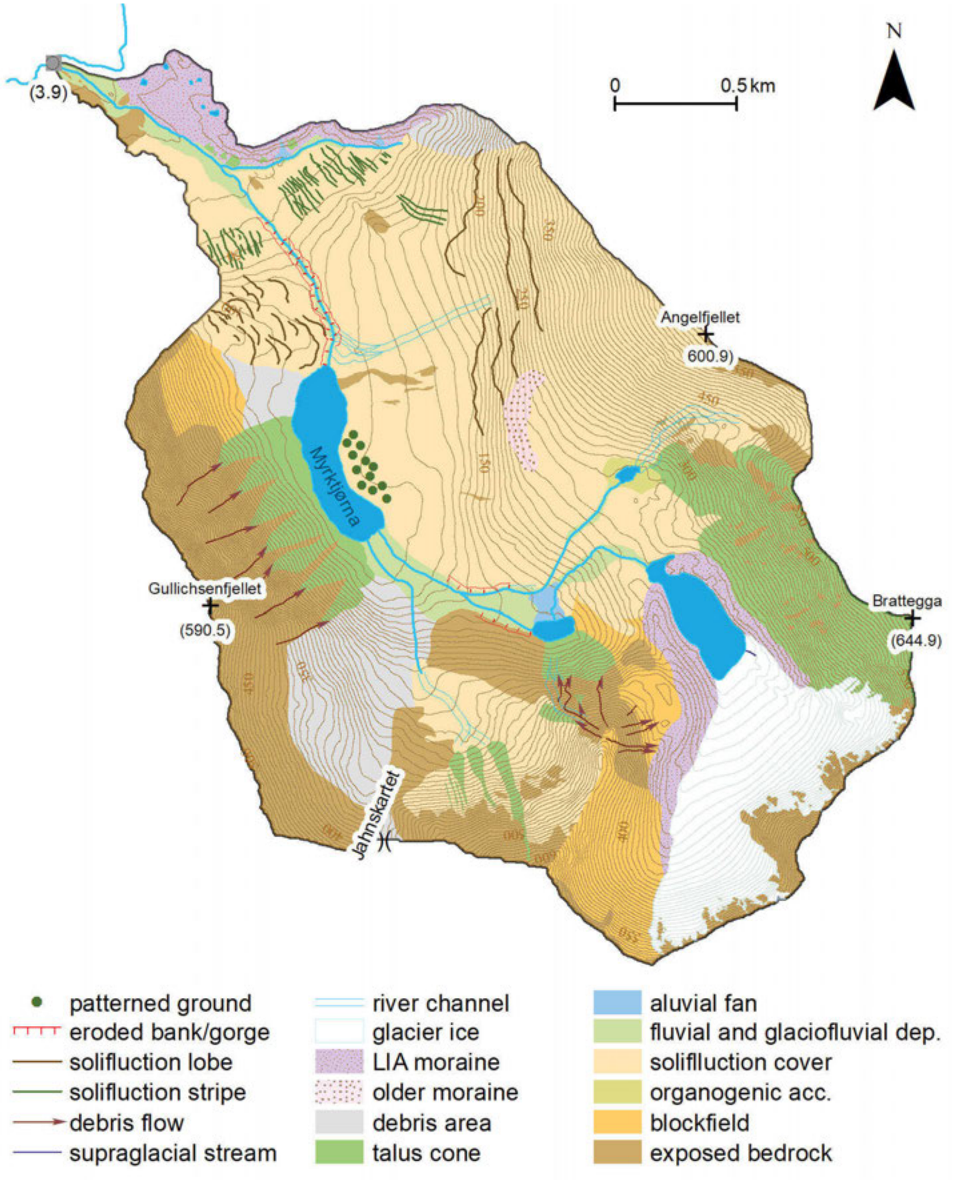

Fig. 4. Geomorphological map of the Bratteggelva catchment.

loss and overburden show relative values due to imperfections in the DEMs. The resulting values are unrealistic, nevertheless, we decided to show the result to demonstrate morphologically active zones. In the orthomosaic of Myrktjørna (Fig. 5), there is visible deposited slope material below the water surface on both banks of the Myrktjørna lake. A well-developed alluvial fan (Fig. 7D) is located right above the middle lake, coinciding with the first slight flattering of the

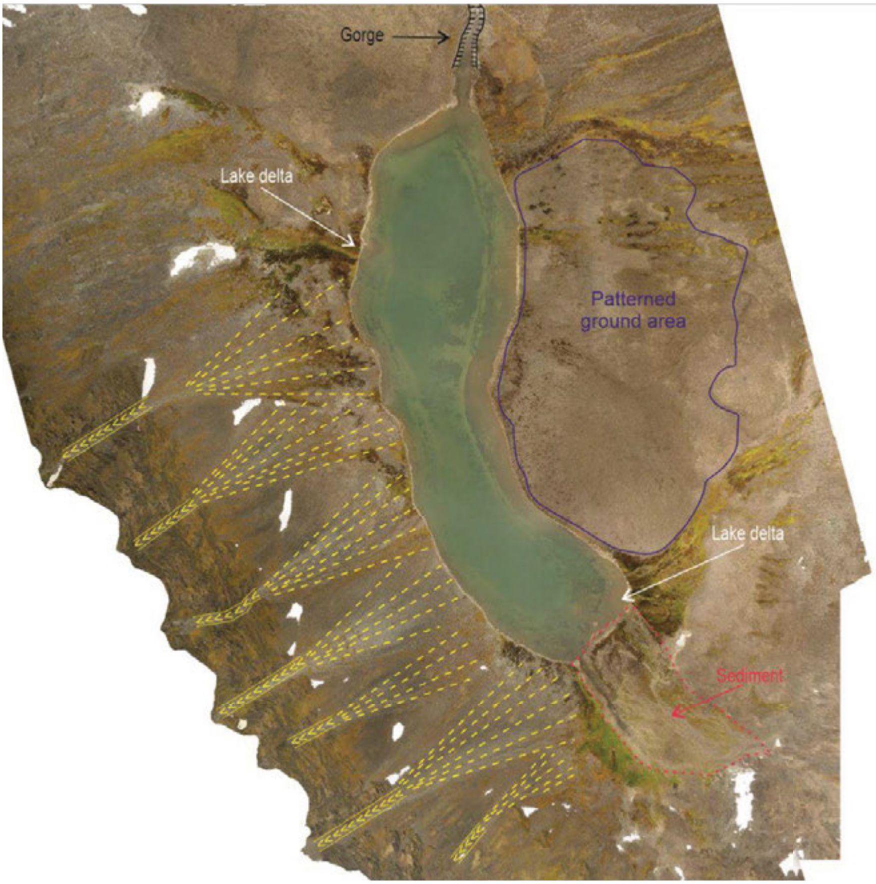

Fig. 5. Orthomosaic of the vicinity of Myrktjørna lake with indicated geomorphological forms.

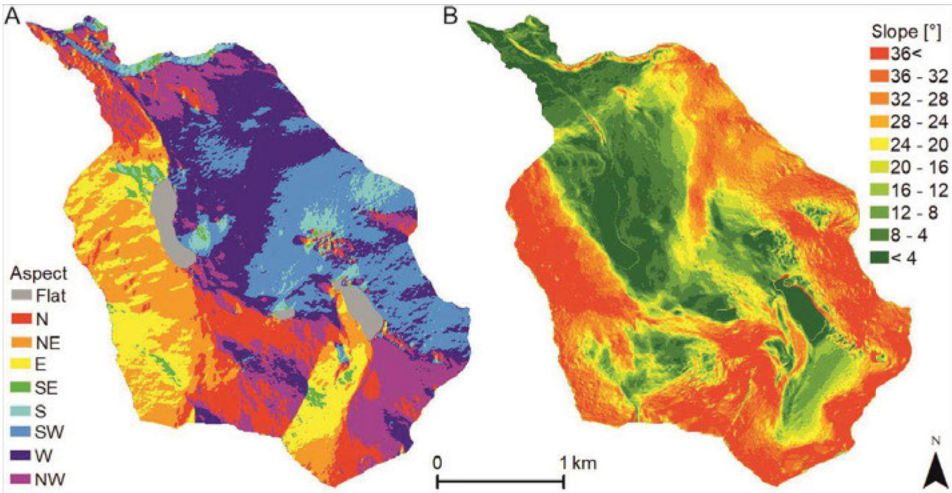

Fig. 6. Aspect (**A**) and slope (**B**) in the Bratteggelva catchment, based on digital elevation model.

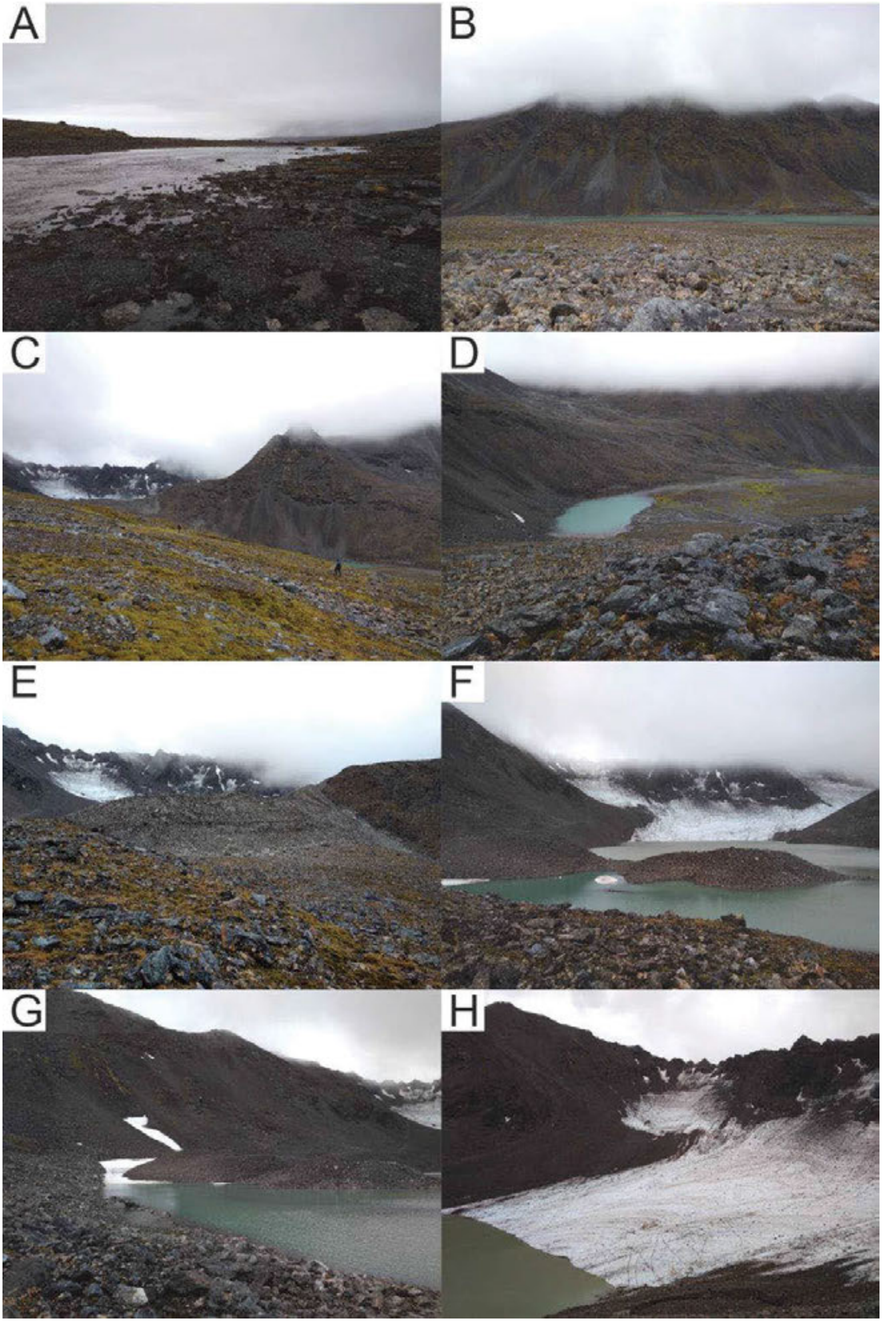

Fig. 7. Photographs from the fieldwork in 2018: **A** - the Myrktjørna lake; **B** - talus cones; **C** - view from Anglefjellet slope of the upper part of the Bratteggelva catchment; **D** - view of the middle lake; **E** - the LIA moraine of Bratteggbreen; **F** - view of the Bratteggbreen with the glacial lake and moraines; **G** - view of the Eastern side of the Bratteggbreen moraines and the slopes above Bratteggbreen; **H** - Bratteggbreen in 2018.

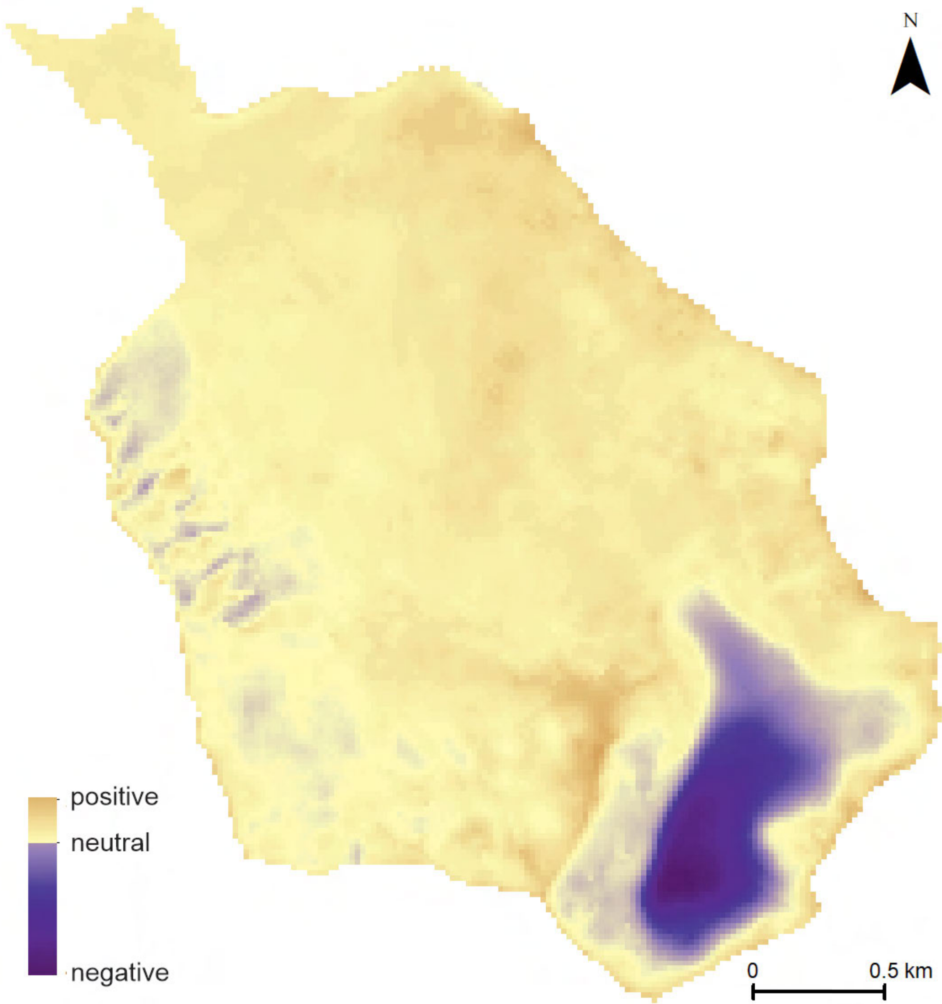

Fig. 8. Elevation change between years 1936 and 2011, based on 20x20 m resolution DEMs from 1936 (Geyman *et al.* 2022b) and 2011 (Norwegian Polar Institute 2014b).

ground from the river efflux. The lake is surrounded by terminal and lateral moraines (Figs. 7E to 7H) composed of different-sized rocks. Inside the eastern lateral moraine, an ice core was observed. Most of the frontal parts of the moraines are progressively sprouted with lichens and mosses (Fig. 7E).

Activity of geomorphological processes and slope cover deposits. — Little is known about slope processes in the Bratteggelva catchment as no continuous monitoring has been carried out therein. Nevertheless, the Myrktjørna lake shallowing and the presence of a cascade (Fig. 3A), which has a large influence on river debris transport, indicates their activity. The slope deposits are mainly composed of eroded bedrock, and thus consist of mica schists, quartzites or amphibolites.

The NDVI analysis reveals a positive change in vegetation growth over the last 45 years (Fig. 9). The mean NDVI value has successively grown from −0.21 in 1976 to 0.17 in 2020 (Table 1). The results for 2020 highlight the locations of water flow and stagnation and these locations provide the best environment for further vegetation growth. Clouds and shadows present in satellite images influence the spectral response of the land cover (Li *et al*. 2007; Peng *et al.* 2016; Xue *et al.* 2018; Yang *et al.* 2022) especially in uneven terrain (Burgess *et al.* 1995; Yang *et al.* 2022), impeding the land-use classification (Anderson *et al.* 2016; Karlsen *et al.* 2021). As the western slopes of the Bratteggelva catchment are often in a shadow, this data was not included during analysis. This is most pronounced for 2020, when the presence of a cloud highly influences NDVI's extreme positive and negative values, thus resulting in a much higher mean value than expected. NDVI statistics for analysed years are presented in Table 1.

Table 1.

Normalized Difference Vegetation Index minimal, maximal and mean values for the years 1976, 1980, 1990, 2010 and 2020.

Year	Minimal	Maximal	Mean
1976	−0.92	0.09	−0.19
1980	−0.80	0.11	−0.12
1990	−0.18	0.36	0.03
2010	−0.18	0.42	0.09
2020	−1	1	0.19

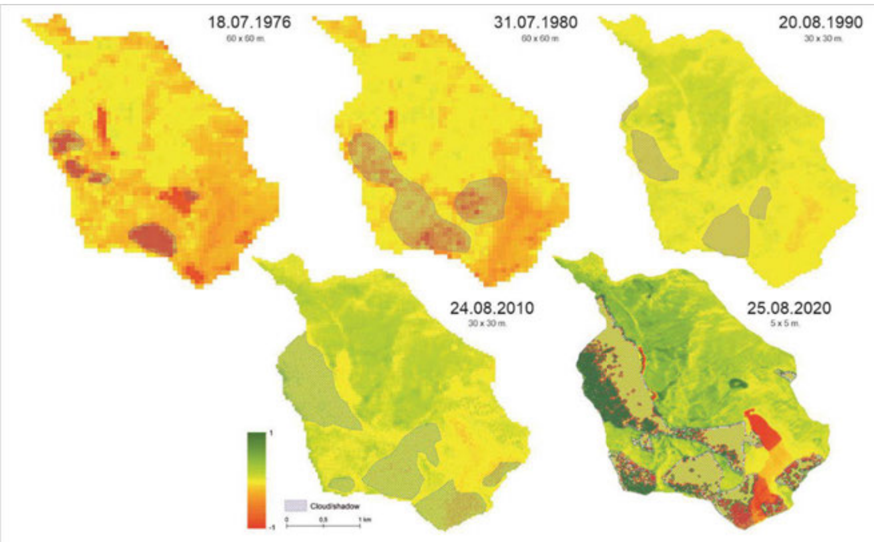

Fig. 9. The Normalized Difference Vegetation Index for the years 1976, 1980, 1990, 2010 and 2020 with marked cloud/shadow coverage excluded from the analysis in the Bratteggelva catchment.

The highest values are observed on eastern slopes where the southern aspect prevails. The flattened area in the catchment's centre is also a place where vegetation is expanding. Organogenic accumulation area is not well presented in the years 1976 and 1980 as the spatial resolution of satellite images, thus the NDVI, is insufficient for its size. In the 1990, 2010 and 2020 images, the area can be distinguished and a gradual increase in the NDVI value can be observed. Hence, environmental conditions at that location were favourable for plant expansion.

Glacial retreat since the Little Ice Age. — The areal extent of Bratteggbreen has decreased by 60–68% since the end of the LIA. Currently, the glacier covers 3.76% (0.28 km^2) of the catchment area but during the LIA it occupied *ca.* 11.8%. The glacier front has, since the end of the LIA (1936–2021) retreated *ca.* 600 m, *i.e.*, 5.8 m per year, and experience a significant surface lowering (Figs. 8 and 10). In parallel, a glacial lake has formed. As it is not

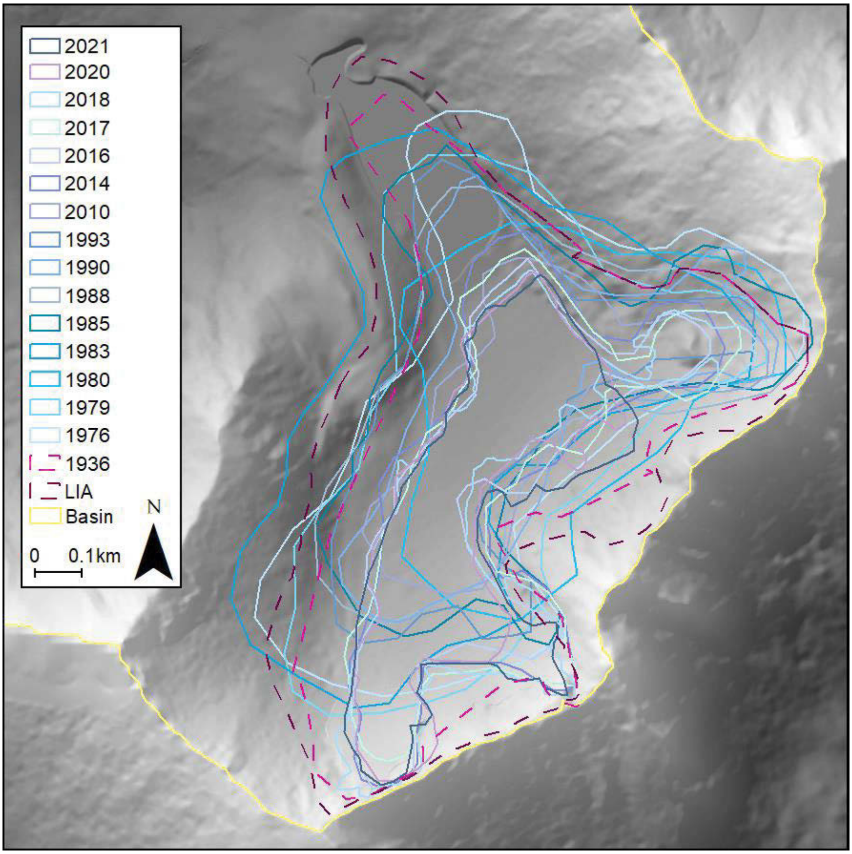

Fig. 10. Bratteggbreen areal change since 1975. Based on satellite images for years 1976–2017 Landsat, source: www.earthexplorer.usgs.gov/; 2018–2021 Sentinel, source: https://apps.sentinel-hub.com/eo-browser/ and based on Geyman *et al.* (2022b) for year 1936. Some shifts are caused by offsets of satellite images and their lower resolution.

visible in the photo from 1936, we can assume that it developed simultaneously with glacier retreat. The terminal moraines represent the maximum extent of Bratteggbreen from the LIA (Fig. 10). The frontal moraines do not seem to have changed its size in the last *ca.* 80 years but rock fall material sourced from the slopes above has been progressively deposited on them (Figs. 7F and 7G). Since 1936, the glacier area has gradually decreased, and is currently at its minimum since the LIA. Between 2018 and 2020, the northeastern part of the glacier got isolated. On the glacier surface, single weathered rocks alternating with small holes 1–2 m wide are visible, from which meltwater channels originate. In the lower part of the glacier, meandering supraglacial streams and glacial ice lamination occur. Where the supraglacial stream flow enters the proglacial lake, a small delta is formed. The oldest known photograph of the glacier is from 1918, when the Norwegian Svalbard Expedition, led by Adolf Hoel, surveyed in the Hornsund region (https://bildearkiv.npolar.no/fotoweb/archives/, Filename: NBR9201_05574, 1918, The Norwegian Polar Institute photo archive). In the 1918 photograph, the glacier front extends just beyond the LIA moraines.

The moraine-like form, marked as 'older moraine' in Fig. 4, may mark the glacier's maximum extent from its former advance. The organogenic accumulation area (Fig. 4) is the witness of that previous glacial advance, with a small (0.004 km^2) lake remaining. That area is also visible in the aerial photographs from 1936 (Fig. 11).

Regional context and future predictions

Bratteggbreen LIA moraines will probably change their current shape due to the melting of buried ice (Midgley *et al.* 2018). The slightly curved, convex form was named "the older moraine", given its shape which is similar to such forms. Its location suggests a linkage with Bratteggbreen or with a small glacier, which remnant is the area of organogenic accumulation. However, the old moraine is the only evidence of a potential pre-LIA glacial advance. The landform is similar to other examples of subtle, potential pre-LIA moraines in Svalbard (Farnsworth *et al.* 2018).

The catchment areas with elevation higher than *ca.* 100 m a.s.l., have high values of slope (>30°) favorable for rock fall, which is common on Svalbard (de Haas *et al.* 2015) and subsequent deposition in the lower parts, resulting in the growth of talus cones (Jahn 1967, 1976; Åkerman 1984; de Haas *et al.* 2015). In the permafrost underlined catchments, water flow is immediate, but with a deepening of the active layer, water absorption is increasingly important. Tananaev and Lotsari (2022) demonstrate the effects of climate warming as an increase in rainfall erosion and both a decrease and increase in soil erosion on hillslopes, due to sparser vegetation cover caused by physical permafrost disturbance. The presented geomorphological map may be used in the future to

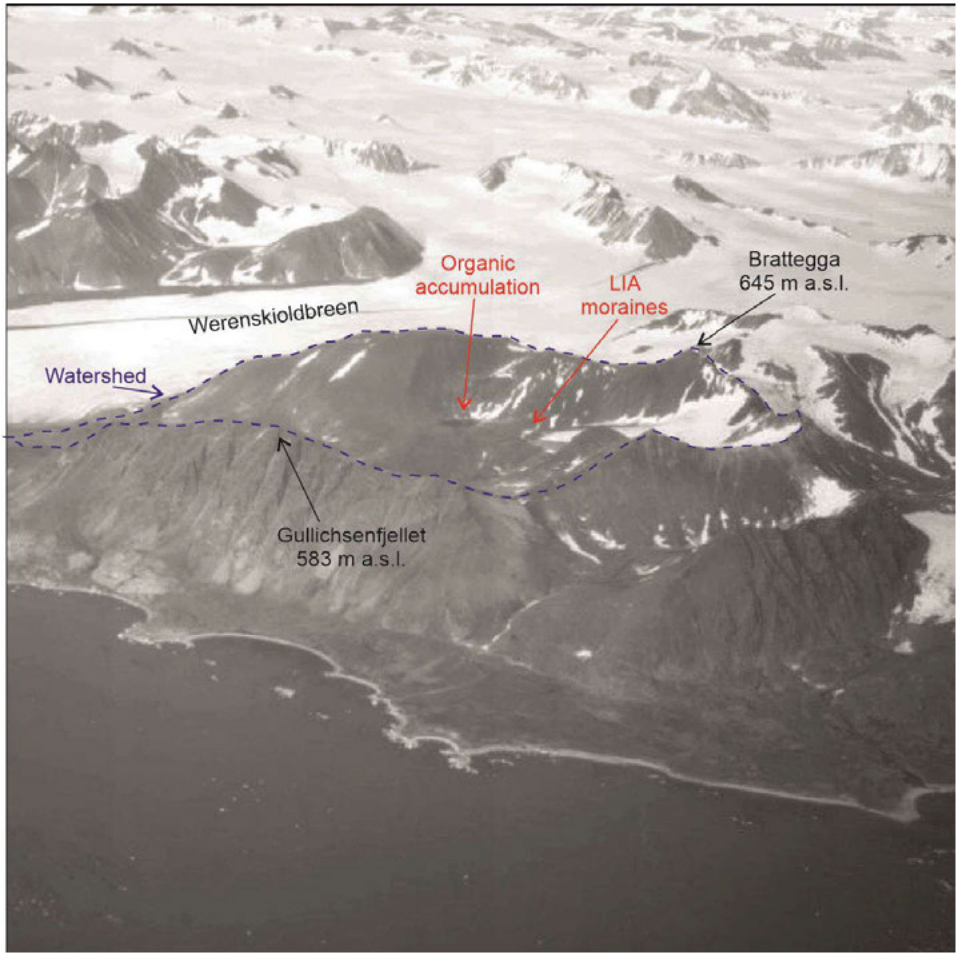

Fig. 11. Aerial photo of the Bratteggelva catchment from 1936, modified after Geyman *et al.* (2022b).

track environmental changes in a spatiotemporal approach (Chandler *et al.* 2018; Allaart *et al.* 2021) and to monitor the activity of slope processes.

Our results are comparable to similar research conducted near glaciers with area <5 km^2 in northwest Svalbard with negative net mass balance in the last *ca.* 30 years of the 20th century (Hagen *et al.* 2003). A study carried out by Huss and Fisher (2016) on mountain glaciers, with an area of <0.5 km^2, suggests that their sensibility to changes in precipitation and temperature does not differ much compared with larger ice masses. However, their morphometric features, such as slope, elevation and presence of debris on ice surface results in large sensibility. The Bratteggbreen fits into the above-mentioned trend with its predominantly gentle slope, with mean value of 15° and 37° at most, supraglacial debris and altitude. Single rocks laying on the glacier's surface blend into the glacier, accelerating its melting (Conway *et al.* 1996; Hansen and Nazaranko 2004; Vacco *et al.* 2010). It is predicted that ice volume in the High Arctic will decrease drastically in the near future and mountain glaciers will likely be the first glaciers to vanish (Huss and Fisher 2016; Małecki 2022). Based on our results, we expect Bratteggbreen to follow this trend.

Svalbard glaciers have low elevations, with a glacier hypsometry peak (area-elevation distribution) at *ca.* 450 m a.s.l. and *ca.* 60% of Svalbard glaciers located at lower altitudes (Noël *et al.* 2020). Since 1985, the average equilibrium line altitude (ELA) has increased from 350 ± 60 m a.s.l. to 440 ± 80 m a.s.l., accelerating glacier ablation and lowering their refreezing capacity (Noël *et al.* 2020). The Bratteggbreen hypsometry (Fig. 1) is situated between 250 and 550 m a.s.l, and thus, a major part of the glacier lies below Svalbard's average ELA. As only 4 satellite images were captured before 1985, it is hard to say if the shift in ELA influenced Bratteggbreen. Noteworthy, satellite images taken before 1985 had the lowest resolution. This could influence the precision of tracing Bratteggbreen areal decrease. Nevertheless, in the last 40 years, clear decrease in glacier area and frontal retreat can be noticed. Recent fast glacial retreat, and the high probability of the glacier vanishing in this small catchment, will lead to high sediment release into the catchment (Ballantyne 2002). This will be enhanced by the steep slopes of glaciers, resulting in greater sediment release (Hooke 2000; Ballantyne 2002). In smaller catchments, permafrost perturbance results in intensified transport of particles (Tananaev and Lotsari 2022), thus sediment yield from the catchment will increase in the future. On the other hand, the proglacial lake in front of Bratteggbreen may serve as a sediment trap and slow down sediment release from the upper part of the catchment (Kavan *et al.* 2022).

The NDVI analysis aimed to show expected growth of vegetation for almost 50 years. For the oldest data, where image resolution was 60 m, the probability of data generalization was greater mainly in smaller research areas. Modern NDVI values, with high resolution, may help with tracing surface and shallow near-surface groundwater runoff. Water flow paths in thawing permafrost conditions and increasing rainfall events for 2020 are visible in Fig. 9. As solifluction takes place in the majority of the Bratteggelva catchment (Fig. 4), we could expect its influence on plant growth (Kemppinen *et al.* 2022). At low levels of movement, solifluction has a positive effect on plant growth but a negative at higher rates (Kemppinen *et al.* 2022). As we mentioned, no continuous monitoring of slope processes is carried out in the catchment, but we believe its rate may be estimated by a more detailed analysis of NDVI during summer periods. On the other hand, plant size and leaf area, which are used for NDVI analysis, are negatively impacted by cryoturbation (Kemppinen *et al.* 2022). As fluvial processes are likely to increase due to rainfall reinforcement (Owczarek *et al.* 2014; Hanssen-Bauer *et al*. 2019), we expect the leaf area and plant size effect to play a role also in the Bratteggelva catchment soon, similar to observations by Kemppinen *et al.* (2022). Our results point to vegetation growth within the catchment, but depending on how environmental changes occur in the near future, this trend may vary, and it is worth future monitoring, preferably with fieldwork.

Further climate warming in the Arctic is expected (Hanssen-Bauer *et al*. 2019). In the area of this study, Bratteggbreen will likely continue retreat and contribute abundant meltwater, resulting in significant hydrological changes within the catchment. We expect the proglacial lake to increase in size and gradually fill in the cirque after Bratteggbreen disappears entirely. Large changes will occur in the river regime as it will be more dependent on rain and snowfall events and thawing permafrost, increasing thickness of the active layer (Isaksen *et al*. 2022). Glacial retreat and eventual disappearance will highly influence river discharge (Owczarek *et al.* 2014), affecting lake water supply, which is already evidenced by shallowing of Myrktjørna. We expect decreasing permafrost thickness and an increase in the number of rainfall events to accelerate slope processes in Bratteggdalen, similar to elsewhere around Svalbard (Hanssen-Bauer *et al*. 2019). Talus cones will continue to develop as the DoD at the Gullichsenfjellet slope showed relative loss and gain of the surface. Debris flows are expected to occur at the Gullichsenfjellet slope, as it is of northeast aspect (Åkerman 1984, 1987). Our NDVI analyses show that the Bratteggelva catchment has become increasingly vegetated during the past 40 years and we expect the trend to continue as a consequence of the ongoing climate change (Hanssen-Bauer *et al*. 2019).

Conclusions

Our study provides data about the effects of climate change in a small (<10 km^2) Arctic catchment and shows how fast changes are reflected in its geosystem. Our results highlight changes in the Bratteggelva catchment since the end of the LIA. The areal extent of Bratteggbreen has decreased 60–68%, the glacier margin has retreated 600 m at the rate of 5.8 m/year, a proglacial lake has formed, and the vegetation cover has expanded, *i.e.*, the Normalized Difference Vegetation Index mean value increased from −0.19 to 0.19 in 45 years. Slope processes are active and expected to increase in the level of activity due to the ongoing climate change. The river regime will likely change due to glacier melting, predicted rainfall increase and permafrost thawing.

Acknowledgements. — Digital elevation models were provided by the Polar Geospatial Center under NSF-OPP awards 1043681, 1559691, and 1542736. This study was part of the research project *Spatial and temporal controls on active layer dynamics in an Arctic mountain valley*, no. 2015/19/D/ST10/02869 of the National Science Centre, Poland. We thank Helen Dulfer for valuable language revision. Finally, we would like to thank Lis Allaart and Wiesław Ziaja for constructive reviews.

References

Åkerman J. 1984. Notes on talus morphology and processes in Spitsbergen. *Geografiska Annaler Series A, Physical Geography* 66: 267–284. doi: 10.1080/04353676.1984.11880115

Åkerman J. 1987. Periglacial forms of Svalbard: a review. *In*: Boardman J. (ed.) *Periglacial processes and landforms in Britain and Ireland.* Cambridge University Press, Cambridge: 9–25.

Allaart L., Schomacker A., Håkansson L.M., Farnsworth W.R., Brynjólfsson S., Grumstad A. and Kjellman S.E. 2021. Geomorphology and surficial geology of the Femmilsjøen area, northern Spitsbergen. *Geomorphology* 382: 107693. doi: 10.1016/j.geomorph.2021.107693

Anderson H.B., Nilsen L., Tømmervik H., Karlsen S.R., Nagai S. and Cooper E.J. 2016. Using ordinary digital cameras in place of near-infrared sensors to derive vegetation indices for phenology studies of High Arctic vegetation. *Remote Sensing* 8: 847. doi: 10.3390/rs8100847

Ballantyne C.K. 2002. A general model of paraglacial landscape response. *The Holocene* 12: 371–376. doi: 10.1191/0959683602hl553fa

Bhatt U.S., Walker D.A., Raynolds M.K. Walsh J.E., Bieniek P.A., Cai L., Comiso J.C., Epstein H. E., Frost G.V., Gersten R., Hendricks A.S., Pinzon J.E., Stock L. and Compton J.T. 2021. Climate drivers of Arctic tundra variability and change using an indicators framework. *Environmental Research Letters* 16: 055019. doi: 10.1088/1748-9326/abe676

Brázdil R., Chmal H., Kida J., Klementowski J., Konečný M., Pereyma J., Piasecki J., Prošek P., Sobik M. and Szczepankiewicz-Szmyrka A. 1988. *Results of investigations of the geographical research expedition Spitsbergen 1985*. Univerzita J. E. Purkyně in Brno, Brno.

Burgess D.W., Lewis P. and Muller J.-P.A.L. 1995. Topographic effects in AVHRR NDVI data. *Remote Sensing of Environment* 54: 223–232. doi: 10.1016/0034-4257(95)00155-7

Chandler B.M.P., Lovell H., Boston C.M., Lukas S., Barr I.D., Benediktsson Í.Ö., Benn D.I., Clark C.D., Darvill C.M., Evans D.J.A., Ewertowski M.W., Loibl D., Margold M., Otto J.-C., Roberts D.H., Stokes C.R., Storrar R.D. and Stroeven A.P. 2018. Glacial geomorphological mapping: a review of approaches and frameworks for best practice. *Earth-Science Reviews* 185: 806–846. doi: 10.1016/j.earscirev.2018.07.015

Christiansen H.H., Etzelmüller B., Isaksen K., Juliussen H., Farbrot H., Humlum O., Johansson M., Ingeman-Nielsen T., Kristensen L., Hjort J., Holmlund P., Sannel A.B.K., Sigsgaard C., Åkerman H.J., Foged N., Blikra L.H., Pernosky and M.A. and Ødegård R.S. 2010. The thermal state of permafrost in the Nordic area during the International Polar Year 2007–2009. *Permafrost and Periglacial Processes* 21: 156–181. doi: 10.1002/ppp.687

Christiansen H.H., Gilbert G.L., Demidov N., Guglielmin M., Isaksen K., Osuch M. and Boike J. 2019. Permafrost temperatures and active layer thickness in Svalbard during 2017/2018 (PermaSval). *SESS Report 2019 – The State of Environmental Science in Svalbard*: 237–249.

Conway H., Gades A. and Raymond C. F. 1996. Albedo of dirty snow during conditions of melt. *Water resources research* 32: 1713–1718. doi: 10.1029/96WR00712

Czerny J., Kieres A., Manecki M. and Rajchel J. 1993. Geological map of the SW part of Wedel Jarlsberg Land, Spitsbergen 1:25000. Manecki A. (ed.) Institute of Geology and Mineral Deposits, University of Mining and Metallurgy. Cracow: 1–61.

De Haas T., Kleinhans M., Carbonneau P., Rubensdotter L. and Hauber E. 2015. Surface morphology of fans in the high-Arctic periglacial environment of Svalbard: Controls and processes. *Earth-Science Reviews* 146: 163–182. doi: 10.1016/j.earscirev.2015.04.004

Dudek J. and Pętlicki M. 2021. Unlocking archival maps of the Hornsund fjord area for monitoring glaciers of the Sørkapp Land peninsula, Svalbard. *Earth System Science Data Discuss [preprint]*. doi: 10.5194/essd-2021-76

Dugan H.A., Lamoureux S.F., Lafrenière M.J. and Lewis T. 2009. Hydrological and sediment yield response to summer rainfall in a small high Arctic watershed. *Hydrological Processes* 23: 514–1526. doi: 10.1002/hyp.7285

Eckerstorfer M. and Christiansen H.H. 2011. The “High Arctic Maritime Snow Climate” in Central Svalbard. *Arctic, Antarctic, and Alpine Research* 43: 11–21. doi: 10.1657/1938-4246-43.1.11

Fang M., Li X., Chen H.W. and Chen D. 2022. Arctic amplification modulated by Atlantic Multidecadal Oscillation and greenhouse forcing on multidecadal to century scales. *Nature Communications* 13: 1865. doi: 10.1038/s41467-022-29523-x

Farnsworth W.R., Ingólfsson Ó., Retelle M., Allaart L., Håkansson L.M. and Schomacker A. 2018. Svalbard glaciers re-advanced during the Pleistocene–Holocene transition. *Boreas* 47: 1022–1032. doi: 10.1111/bor.12326

Francis J.A. and Vavrus S.J. 2012. Evidence linking Arctic amplification to extreme weather in mid-latitudes. *Geophysical Research Letters* 39: L06801. doi: 10.1029/2012GL051000,

Geyman E.C., van Pelt W.J.J., Maloof A.C., Aas H.F. and Kohler J. 2022a. Historical glacier change on Svalbard predicts doubling of mass loss by 2100. *Nature* 601: 374–379. doi: 10.1038/s41586-021-04314-4

Geyman E., van Pelt W., Maloof A., Aas H.F. and Kohler J. 2022b. 1936/1938 DEM of Svalbard [Data set]. Norwegian Polar Institute. doi: 10.21334/npolar.2021.f6afca5c

Gilewska S. 1968. Project of the unified key to the detailed geomorphological map of the world. *Folia Geographica. Series Geographica-Physica* 2. Polska Akademia Nauk. Komisja Geograficzna, Kraków.

Goosse H., Kay J.E., Armour K.., Bodas-Salcedo A., Chepfer H., Docquier D., Jonko A., Kushner P.J., Lecomte O., Massonnet F., Park H.-S., Pithan F., Svensson G. and Vancoppenolle M. 2018. Quantifying climate feedbacks in polar regions. *Nature Communications* 9: 1919. doi: 10.1038/s41467-018-04173-0

Górniak D., Marszałek H. and Jankowska K. 2012. Environmental conditions and composition of microbial assemblages in the postglacial lotic-lenitic system of the Arctic Brattegg Valley (West Spitsbergen). *Streszczenia referatów i posterów. XXXIV Sympozjum Polarne.* Sosnowiec: 30 (in Polish).

Górniak D., Marszałek H., Jankowska K. and Dunalska J. 2015. Bacterial community succession in an Arctic lake-stream system (Brattegg Valley, SW Spitsbergen). *Boreal environment research* 21: 115–133.

Hagen J.O., Kohler J., Melvold K. and Winther J. G. 2003. Glaciers in Svalbard: Mass balance, runoff and freshwater flux. *Polar Research* 22: 145–159.

Hansen J. and Nazarenko L. 2004. Soot climate forcing via snow and ice albedos. *Proceedings of the national academy of sciences* 101: 423–428. doi: 10.1073/pnas.2237157100

Hanssen-Bauer I., Førland E.J., Hisdal H., Mayer S., Sandø A.B. and Sorteberg A. 2019. Climate in Svalbard 2100 — a knowledge base for climate adaptation. Norwegian Centre for Climate Services Reports. The Norwegian Centre for Climate Services (NCCS).

Hooke R.-LeB. 2000. Toward a uniform theory of clastic sediment yield in fluvial systems. *Geological Society of America Bulletin* 112: 1778–1786. doi: 10.1130/00167606(2000)112<1778:TAUTOC>2.0.CO;2

Huss M. and Fischer M. 2016. Sensitivity of very small glaciers in the swiss alps to future climate change. *Frontiers in Earth Science* 4: 34. doi: 10.3389/feart.2016.00034

Ignatiuk D., Błaszczyk M., Budzik T., Grabiec M., Jania J.A., Kondracka M., Laska M., Małarzewski Ł. and Stachnik Ł. 2022. A decade of glaciological and meteorological observations in the Arctic (Werenskioldbreen, Svalbard). *Earth System Scientific Data* 14: 2487–2500. doi: 10.5194/essd-14-2487-2022

Isaksen K., Lutz J., Sørensen A.M., Godøy Ø., Ferrighi L., Eastwood S. and Aaboe S. 2022. Advances in operational permafrost monitoring on Svalbard and in Norway. *Environmental Research Letters* 17: 095012. doi: 10.1088/1748-9326/ac8e1c

Jahn A. 1967. Some features of mass movements on Spitsbergen slopes. *Geografiska Annaler* A 49: 213–225.

Jahn A. 1976. Contemporaneous geomorphological processes in Longyeardalen, Vestspitsbergen (Svalbard). *Biuletyn Peryglacjalny* 26: 253–268.

Jania J. 1988. Dynamic glacial processes in south Spitsbergen: in the light of photointerpretation and photogrammetric research. *Prace naukowe Uniwersytetu Śląskiego w Katowicach* 955: 49 (in Polish).

Johansen B. and Tømmervik H. 2014. The relationship between phytomass, NDVI and vegetation communities on Svalbard. *International Journal of Applied Earth Observation and Geoinformation* 27: 20–30. doi: 10.1016/j.jag.2013.07.001

Jokiel B., Kasprzak M. and Klementowski J. 2012. The role of nivation in the morphogenesis of the slopes of Wedel Jarlsberg Land (SW Spitsbergen) as an example of Schmidt hammer rock strength measurements. *In:* Krawczyk E. and Styczyńska A. (eds.) *Streszczenia referatów i posterów. XXXIV Sympozjum Polarne*, Sosnowiec: 35 (in Polish).

Karczewski A. 1984. Conceptualization and preparation of a geomorphological map of the Hornsund Fjord area (SW Spitsbergen). *XI Sympozjum Polarne. Referaty i sprawozdania.* Poznań: 60–64 (in Polish).

Karlsen S., Stendardi L., Tømmervik H., Nilsen L., Arntzen I. and Cooper E. J. 2021. Time-series of cloud-free sentinel-2 ndvi data used in mapping the onset of growth of central Spitsbergen, Svalbard. *Remote Sensing* 13: 3031. doi: 10.3390/rs13153031

Kasprzak M. 2015. High-resolution electrical resistivity tomography applied to patterned ground, Wedel Jarlsberg Land, south-west Spitsbergen. *Polar Research* 34: 25678. doi: 10.3402/polar.v34.25678

Kasprzak M. 2020. Seawater intrusion on the Arctic coast (Svalbard): The concept of onshore-permafrost wedge. *Geosciences* 10: 1–11. doi: 10.3390/geosciences10090349

Kavan J., Wieczorek I., Tallentire G.D., Demidionov M., Uher J. and Strzelecki M.C. 2022. Estimating suspended sediment fluxes from the largest glacial lake in Svalbard to fjord system using Sentinel-2 Data: Trebrevatnet case study. *Water* 14: 1840. doi: 10.3390/w14121840

Kemppinen J., Niittynen P., Happonen K., le Roux P.C., Aalto J., Hjort, J., Maliniemi T., Karjalainen O., Rautakoski H. and Luoto M. 2022. Geomorphological processes shape plant community traits in the Arctic. *Global Ecology and Biogeography* 31: 1381–1398. doi: 10.1111/geb.13512

Kowalska A. and Sroka W. 2008. Sedimentary environment of the Nottinghambukta delta, SW Spitsbergen. *Polish Polar Research* 29: 245–259.

Lafrenière M.J. and Lamoureux S.F. 2019. Effects of changing permafrost conditions on hydrological processes and fluvial fluxes. *Earth-Science Reviews* 191: 212–223. doi: 10.1016/j.earscirev.2019.02.018

Lamoureux S.F., Lafrenière M.J. and Favro E.A. 2014. Erosion dynamics following localized permafrost slope disturbances. *Geophysical Research Letters* 41: 5499–5505. doi: 10.1002/2014GL060677

Li Y., Gong P. and Sasagawa T. 2007. Integrated shadow removal based on photogrammetry and image analysis, *International Journal of Remote Sensing* 26: 3911–3929. doi: 10.1080/01431160500159347.

Majka J., Czerny J., Mazur S., Holm D.K. and Manecki M. 2010. Neoproterozoic metamorphic evolution of the Isbjørnhamna Group rocks from south-western Svalbard. *Polar Research* 29: 250–264. doi: 10.3402/polar.v29i3.6086

Małecki J. 2022. Recent contrasting behaviour of mountain glaciers across the European High Arctic revealed by ArcticDEM Data. *Cryosphere* 16: 2067–2082. doi: 10.5194/tc-16-2067-2022

Manecki A., Czerny J., Kieres A., Manecki M. and Rajchel J. 1993. Geological Map of the SW part of Wedel Jarlsberg Land, Spitsbergen, 1:25 000. Akademia Górniczo-Hutnicza, Kraków.

Markham B.L. and Barker J.L. 1983. Spectral characterization of the Landsat-4 MSS sensors. *Photogrammetric Engineering and Remote Sensing* 49: 811–833. doi: 0099-1112/83/4906-0811$02.25/

Marszałek H. and Górniak D. 2017. Changes in water chemistry along the newly formed High Arctic fluvial–lacustrine system of the Brattegg Valley (SW Spitsbergen, Svalbard). Environmental Earth Sciences 76: 449. doi: 10.1007/s12665-017-6772-9

Marszałek H. and Wąsik M. 2013. Some physico-chemical features of water in suprapermafrost zone in the Hornsund region (SW Spitsbergen). *Biuletyn Państwowego Instytutu Geologicznego* 456: 397–404.

Marszałek H., Staśko S. and Wąsik M. 2013. Estimation of subsurface runoff in the Hornsund region (SW Spitsbergen). *Biuletyn Państwowego Instytutu Geologicznego* 456: 391–396.

Midgley N.G., Tonkin T.N., Graham D.J. and Cook S.J. 2018. Evolution of high-Arctic glacial landforms during deglaciation. *Geomorphology* 311: 63–75. doi: 10.1016/j.geomorph.2018.03.027

Migoń P. and Kasprzak M. 2013. Geographical environment in the vicinity of the Stanisław Baranowski Polar Station – Werenskioldbreen. Geographical environment. Landforms. *In:* Zwoliński Z., Kostrzewski A. and Pulina M. (eds.) *Ancient and modern geosystems of Spitsbergen*. Bogucki Wydawnictwo Naukowe, Poznań: 104–114.

Norwegian Polar Institute. 2014a. Kartdata Svalbard 1:1 000 000 (S1000 Kartdata) [Data set]. Norwegian Polar Institute. doi: 10.21334/npolar.2014.63730e2e

Norwegian Polar Institute. 2014b. Terrengmodell Svalbard (S0 Terrengmodell) [Data set]. Norwegian Polar Institute. doi: /10.21334/npolar.2014.dce53a47

Noël B., Jakobs C.L., van Pelt W.J.J., Lhermitte S., Wouters B., Kohler J., Hagen J.O., Luks B., Reijmer C.H., van de Berg W.J. and van den Broeke M.R. 2020. Low elevation of Svalbard glaciers drives high mass loss variability. *Nature Communications* 11: 4597. doi: 10.1038/s41467-020-18356-1

Owczarek P., Nawrot A., Migała K., Malik I. and Korabiewski B. 2014. Flood-plain responses to contemporary climate change in small High-Arctic basins (Svalbard, Norway). *Boreas* 43: 348–402. doi: 10.1111/bor.12061

Peng Y., He G., Zhang Z., Long T., Wang M. and Ling S. 2016. Study on atmospheric correction approach of Landsat-8 imageries based on 6Smodel and look-up table. *Journal of Applied Remote Sensing* 10: 1–13. doi: 10.1117/1.jrs.10.045006.

Peng X., Zhang T., Frauenfeld O.W., Wang K., Luo D., Cao B., Su H., Jin H. and Wu Q. 2018. Spatiotemporal Changes in Active Layer Thickness under Contemporary and Projected Climate in the Northern Hemisphere. *Journal of Climate* 31: 251–266. doi: 10.1175/JCLI-D-16-0721.1

Pereyma J., Migała K. and Sikora S. 2013. Geographical environment in the vicinity of the Stanisław Baranowski Polar Station – Werenskioldbreen. Geographical environment. Climate. *In:* Zwoliński Z., Kostrzewski A., Pulina M. (eds.), *Ancient and modern geosystems of Spitsbergen*. Bogucki Wydawnictwo Naukowe, Poznań: 118–121.

Piechura J. and Walczowski W. 2009. Warming of the West Spitsbergen Current and sea ice north of Svalbard. *Oceanologia* 51: 147–164. doi: 10.5697/oc.51-2.147

Phiri D., Simwanda M., Salekin S., Nyirenda V.R., Murayama Y. and Ranagalage M. 2020. Sentinel-2 data for land cover/use mapping: A review. *Remote Sensing* 12: 2291. doi: 10.3390/rs12142291

Porter C., Morin P., Howat I., Noh M-J., Bates B., Peterman K., Keesey, S., Schlenk M., Gardiner Judith., Tomko K., Willis M., Kelleher C., Cloutier M., Husby E., Foga S., Nakamura H., Platson M., Wethington M. Jr., Williamson C., Bauer G., Enos J., Arnold G., Kramer W., Becker P., Doshi A., D'Souza C., Cummens P., Laurier F. and Bojesen M. 2018. ArcticDEM. doi: 10.7910/DVN/OHHUKH, Harvard Dataverse, V1 [Access 16.12.2018].

Senderak K. and Wąsowski M. 2016. Chemical weathering of talus slopes: The example of slopes in the Brattegg Valley, SW Spitsbergen. *Studia Geomorphologica Carpatho-Balcanica* 1: 105–122.

Senderak K., Kondracka M. and Gądek B. 2019. Postglacial talus slope development imaged by the ERT method: comparison of slopes from SW Spitsbergen, Norway and Tatra Mountains, Poland. *Open Geoscience* 11: 1084–1097. doi: 10.1515/geo-2019-0084

Serreze M.C. and Barry R.G. 2011. Processes and impacts of Arctic amplification: a research synthesis. *Global Planetary Change* 77: 85–96. doi: 10.1016/j.gloplacha.2011.03.004

Strand S.M., Christiansen H.H., Johansson M., Åkerman J. and Humlum O. 2021. Active layer thickening and controls on interannual variability in the Nordic Arctic compared to the circum-Arctic. *Permafrost and Periglacial Processes* 32: 47–58. doi: 10.1002/ppp.2088

Szafraniec J.E. 2018. Deglaciation rate on southern and western Spitsbergen in the conditions of Arctic amplification. *Polish Polar Research* 39: 77–98. doi: 10.24425/118739

Szponar A. 1989. Deglaciation of Spitsbergen glacier cirques in aqueous and subaqueous conditions. Results of investigations of the Polish Scientific Spitsbergen expeditions Vol. VII, *Acta Universitas Wratislaviensis* 1069: 87–93.

Tananaev N. and Lotsari E. 2022. Defrosting northern catchments: Fluvial effects of permafrost degradation. *Earth-Science Reviews* 228: 103996. doi: 10.1016/j.earscirev.2022.103996

Vacco D.A., Alley R.B. and Pollard D. 2010. Glacier advance and stagnation caused by rock avalanches. *Earth and Planetary Science Letters* 294: 123–130. doi: 10.1016/j.epsl.2010.03.019

Walczowski W. and Piechura J. 2011. Influence of the West Spitsbergen Current on the Local Climate. *International Journal of Climatology* 31: 1088–1093. doi: 10.1002/joc.2338

Wawrzyniak T. and Osuch M. 2020. A 40-year High Arctic climatological dataset of the Polish Polar Station Hornsund (SW Spitsbergen, Svalbard). *Earth System Science Data* 12: 805–815. doi: 10.5194/essd-12-805-2020

Xue L., Yang S., Li Y. and Ma J. 2018. An automatic shadow detection method for high-resolution remote sensing imagery based on polynomial fitting. *International Journal of Remote Sensing* 40: 2986–3007. doi: 10.1080/01431161.2018.1538586

Yang X., Zuo X., Xie W., Li Y., Guo S. and Zhang H. 2022. A correction method of NDVI topographic shadow effect for rugged terrain. *IEEE Journal of Selected Topics in Applied Earth Observations and Remote Sensing* 15: 8456–8472. doi: 10.1109/JSTARS.2022.3193419

Received 29 June 2022
Accepted 21 February 2022